

# Modelling and Analysis of Four-Junction Tandem Solar Cell in Different Environmental Conditions

Mr. Biraju J. Trivedi<sup>1</sup> Prof. Surendra Kumar Sriwas<sup>2</sup>

<sup>1</sup>Research Scholar <sup>2</sup>Assistant Professor

<sup>1,2</sup>Department of Electronics & Communication Engineering

<sup>1,2</sup>Bundelkhand Institute of Engineering College, Jhansi, Uttar Pradesh

**Abstract**—This paper present a MATLAB/Simulink model of a four junction tandem solar cell GaInP/GaAs/GaInAs/Ge for high efficiency. Tandem solar cell means it has more than one junction. The energy band gaps of the sub-cells in a GaInP/ GaAs/ InGaAs/ Ge 4-J tandem solar cell are 1.9 eV, 1.4 eV, 1.1eV and 0.75 eV respectively. In a space applications, generally triple junction from III-V compound semiconductor GaInP/GaAs/Ge is used, because it delivered highest efficiency compare to other commercially available triple junction solar cell. In a multi-junction solar cell, increasing the number of junctions generally offer higher efficiencies. We study here the mathematical model and electrical equivalent circuit of four layer multi-junction solar cell and compare with the triple junction and single junction solar cell and simulation of 4-layer multi-junction solar cell is discussed. We analyzed these models in various environmental conditions such as: solar irradiation, cell's working temperature and concentration of suns. In this we consider three main factors: maximum power (Pmax), open circuit voltage, Short circuit current density of the solar cell. Taking into account the overall effect of solar irradiance and temperature, the model are evaluated, resulted simulated data are presented. It also include the effect on the bandgap of each sub-cells as well as diode reverse saturation current due to variation in the temperature.

**Key words:** Multi-Juncton, Tunnel Diode, Current Density, MATLAB/Simulink

## I. INTRODUCTION

Unlike silicon, the III-V compound semiconductor provide the flexibility to realize multiple solar cells stacked on top of each other following same crystal lattice. The flexibility in band-gap selection provides an unprecedented degree of freedom in solar cell design through metamorphic or lattice-matched configurations based on III-V materials. From the Figure 1, we can clearly see that the multiple solar cells stacked on top of one another in III-V multi-junction solar cells allow a much broader absorption of the incident solar spectrum compared to the conventional single-junction (1J) Si solar cells. The multiple III-V solar cells when connected in series and designed in such a way that they generate the same photo-current, allows linear addition of the voltages from the individual sub-cell resulting in higher conversion efficiencies. The band-gap vs. lattice constant gives an overview of different compound semiconductor alloys that can be made by careful engineering the band-gaps and lattice constants in a device design. The four most readily available semiconductor substrates include Si, Ge, GaAs and InP. This places a constraint on the band-gap and lattice-constant selection for optimal device design, wherein lattice-match structure are desired. The highest efficiency achieved from lattice-matched thin film 1J GaAs and 2J InGaP/GaAs solar cells are 28.8% and 30.8%, respectively at 1-sun [2,3]. A record efficiency of 32.6% at 1000 suns has been

demonstrated for the 2J InGaP/GaAs cell on GaAs substrate. However, experimental realization of high quality epitaxial 3J solar cells comprising of sub-cells with the ideal band-gap combinations has been quite challenging. Utilizing Ge (band-gap = 0.67eV) as the bottom sub-cell in a lattice-matched 3J solar cell configuration, cell efficiency in excess of 40% was demonstrated for the first time by King et al. In search for 1eV bottom sub-cell, the most commonly followed path initially was the integration of 1eV metamorphic InGaAs solar cell in the 3J configuration with lattice matched InGaP and GaAs as the top two sub-cells [4]. Recent works in GaAs solar cell design have achieved great successes in improving performance, by introducing 4 or 5 layers of MJ cells.

MATLAB/Simulink is used for device modelling to focus to optimizing the photovoltaic cell performance. The MATLAB/Simulink software is high level software in which we design the multi-junction solar cells.

## II. STRUCTURE OF MULTI-JUNCTION SOLAR CELL

The introduction of a GaAs sub-cell of 1.4 eV makes better use of the solar spectrum a leads to better efficiency for the GaInP/GaAs/InGaAs/Ge 4-J tandem solar cell. However, it puts forward a high request on the cell structure. There should be a tunnel junction between every two sub-cells, four in total. According to research on GaInP/GaAs/InGaAs 3-J tandem solar cells, solar cells with  $p^{++} \text{AlGaAs}/n^{++} \text{GaAs}$  as tunnel junctions have higher  $V_{oc}$  and then cells with  $p^{++} \text{AlGaAs}/n^{++} \text{GaAs}$  as T-Js. So  $p^{++} \text{AlGaAs}/n^{++} \text{GaAs}$  tunnel junctions are employed in the 4-J tandem solar cells in this paper.

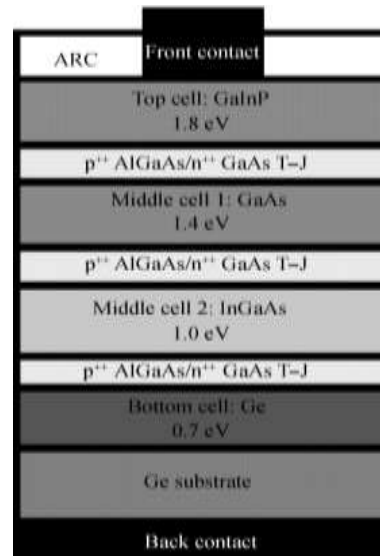


Fig. 1: Four Junction Solar Cell Structure

Figure 1 shows the overall structural diagram of a GaInP/GaAs/InGaAsP/Ge 4-J tandem cell. In consideration of the short diffusion length of the minority carrier and the overall stability of the cell, the thickness of each sub-cell

should be small or recombination should occur before the carriers reach the contact, so that the current density of each sub-cell will be severely reduced. For this, the thickness of each sub-cell thin film is set as GaInP 2 $\mu$ m, GaAs 3 $\mu$ m, InGaAs 4 $\mu$ m, Ge 5 $\mu$ m. Each sub-cell consists of two parts, an n-type emitter and a p-type absorber, to form a p-n junction inside the cell to collect electrons and holes. The thickness of the tunnel junction is set to be 30 nm, so that the tunnel junction can lattice match to the up and down layers, and create good light permeability. For better matching and transmission of the current in sub-cells, each tunnel junction must be a heavily doped p-n junction and the doping concentration should be over 10<sup>19</sup> per cm<sup>3</sup>. The doping level at two sides of the junction even reaches 10<sup>20</sup> per cm<sup>3</sup>. So the resistance of the tunnel junction can be low enough to further reduce the V<sub>oc</sub> loss on it [4].

As can be seen from Fig. 2, the maximum peak tunneling current of AlGaAs/GaAs T-J is 637 A/cm<sup>2</sup>, the relevant effective doping concentration is between 2.5 $\times$ 10<sup>19</sup> and 3.0  $\times$ 10<sup>19</sup> per cm<sup>3</sup>. Here, the conduction offset has two effects: reducing the tunneling barrier and reducing the tunneling width, as shown in Eq. (1), both effects can make the tunneling current increase. So, the conduction offset caused by the tunnel junction's heavy doping has a direct influence on the tunneling current, which is realized by reducing the tunneling barrier and tunneling width [4]. Based on this, the doping concentration of the AlGaAs/GaAs tunnel junction is set as 3.0 $\times$ 10<sup>19</sup> cm<sup>-3</sup>, as heavy as possible to reduce the resistance, increase the tunneling current and thus reduce voltage loss [5].

### III. EXPERIMENTAL PROCEDURE OF COMBINED MJSC

The main objective of this research is to how to analysis the behavior of multi-junction solar cell and how to improve the conversion efficiency of solar cell. There are some steps to check the performance of tandem solar cell.

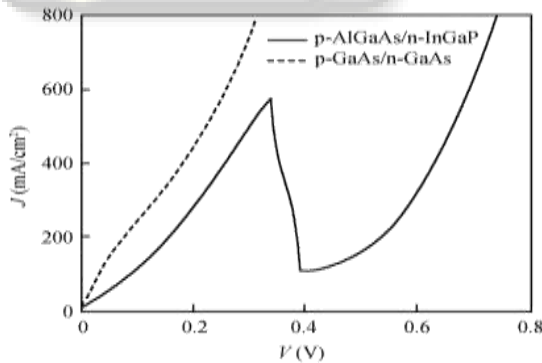


Fig. 2: Characteristics of T-J of solar cell

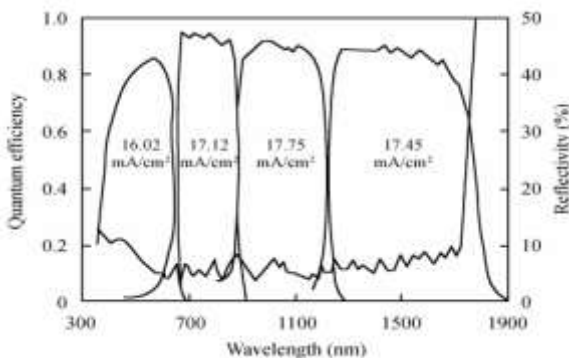


Fig. 3: External quantum Efficiency of Each Sub-cells

Fig. 4 shows two diode model circuit of the most comprehensive equivalent circuits proposed for a single junction solar cell and four layer multi-junction solar cell [6,7]. This circuit model can represent the thermos/optical/electro behaviors of the solar cell across the wide range of received solar irradiance and temperature, if the model parameters determined correctly.

The tunnel junction's material, construction, doping and characteristics, the photoelectric characteristic, light permeability, peak tunneling current characteristics and the influence on the sub-cells are discussed above. Further research on the four junction solar cell influence on the whole cell is made below. On the whole cell's characteristics, MATLAB/Simulink is used to simulate the J-V and P-V curves of the cell. The parameters used in the simulation are shown in Table 1. Table 1 shows the main parameters used in the simulation, other parameters are set as default. Because of the heavy doping of the tunnel junction, defects caused by the heterojunction between tunnel junction and sub-cell are neglected. The resistance of the tunnel junction is also neglected. The curves and parameters are observed under condition of AM0G, 135.3 mW/cm<sup>2</sup>, temperature of 28°C. The current density of each sub-cell shown in Fig. 3 is 16.02, 17.12, 17.75, and 17.45 mA/cm<sup>2</sup>, as a result of the heavily doped tunnel junctions, the current matching of each sub-cell is clear to see[1]. As shown in Fig. 3, each sub-cell's EQE has reached the optimal value of 90%, while the reflectance drops below 10% with the incident light wavelength under 1700 nm.

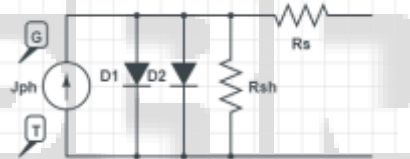


Fig. 4: Equivalent Circuit diagram of two diode model of 1-J solar cell

The fundamental equation of solar cell current can be expressed as [9,10]

$$J_{cell} = J_{ph} - J_{d1} - J_{d2} - \frac{V_{cell} + R_s J_{cell}}{R_p} \quad (1)$$

$$J_{sc} = q \times g \times (L_p + L_n + W) \quad mA \quad (2)$$

$$J_{d1} = J_{sati}(T) \left( \exp \left( \frac{q(V_{cell} + R_s J_{cell})}{n_1 k T} \right) - 1 \right) \quad (3)$$

$$J_{sati} = J_{sati}(T_0) \left( \frac{T}{T_0} \right)^{\frac{3}{n_1}} \exp \left( \left( \frac{q}{n_1 k} \right) \left( \frac{E_g(T_0)}{T_0} - \frac{E_g(T)}{T} \right) \right) \quad (4)$$

$$E_g(T) = E_g(T_0) - \frac{\alpha T^2}{T + \beta} \quad (5)$$

Where J<sub>cell</sub> and V<sub>cell</sub> is the output solar cell current density and voltage, J<sub>ph</sub> is the photon current produced by the solar radiation fall on the solar cell, is approximately equal to short circuit current density J<sub>sc</sub>. J<sub>d1</sub> and J<sub>d2</sub> are the dark current density.

$$V_t = \frac{n \times k \times T}{q} \quad (6)$$

The built in potential V<sub>B</sub> of solar cell, depletion width W, absorption coefficient  $\alpha$ , generation rate g, and reverse saturation current J<sub>s</sub> and open circuit voltage of solar cell can be calculated by using this solar cell equations.

$$V_B = V_t \times \log \frac{N_D}{N_i} \times \frac{N_A}{N_i} \quad (7)$$

$$W = \sqrt{\frac{2 \times \epsilon_0 \times V_B}{q} \left( \frac{N_A + N_D}{N_A \times N_D} \right)} \quad (8)$$

Where  $N_D$ ,  $N_A$ , and  $N_i$  are donor concentration, acceptor concentration and intrinsic concentration of solar cell.

$$\alpha = C \times \sqrt{h \times \vartheta - E_g} \quad (9)$$

$$g = \alpha \times F \times (1 - R_f) \times \exp(-\alpha \times W) \quad (10)$$

$$J_{sc} = q \times g \times (L_p + L_n + W) \quad (11)$$

$$J_s = q \times N_i \times N_i \left( \frac{D_p}{L_p \times N_D} + \frac{D_n}{L_n + N_A} \right) \quad (12)$$

The open circuit voltage  $V_{oc}$ , maximum power  $P_{max}$ , and efficiency of solar cell can be calculated as

$$V_{oc} = V_t \times \log \times \left( \frac{J_{sc}}{J_s} + 1 \right) \quad (13)$$

$$P_{max} = V_{oc} \times J_{sc} \times FF \quad (14)$$

$$\eta = \frac{P_{max}}{P_{in}} = \frac{FF \times V_{oc} \times J_{sc}}{G} \quad (15)$$

The overall current of multi-junction solar cell is minimum current flow from the sub-cells and cell voltage is summation of the sub-cells voltage minus tunnel diode voltage between each sub-cells. Mathematical formulation and equivalent circuit of four layer multi-junction solar cell:

$$J_{cell} = J_{top} = J_{middle1} = J_{middle2} = J_{bottom} \quad (16)$$

$$V_{cell} = V_{top} - V_{TD1} + V_{Middle1} - V_{TD2} + V_{Middle2} - V_{TD3} + V_{Bottom} \quad (17)$$

Where  $J_{top}$ ,  $J_{middle1,2}$ ,  $J_{bottom}$ , are the short circuit current density of top, middle and bottom sub-cells and  $V_{top}$ ,  $V_{middle1,2}$ ,  $V_{bottom}$ , are the open circuit voltages of each sub-cells.

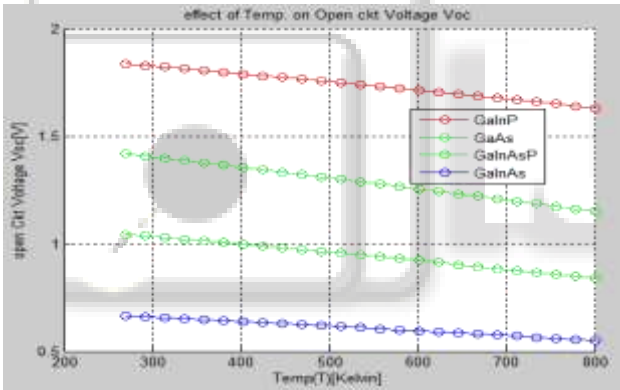


Fig. 5: Effect of Temp. on bandgap of each sub cells

The Tunnel diode current density between sub-cells can be calculated by using these equation

$$J = A \exp \left( - \frac{BE_B^3}{E_F} \right) \left( \frac{E}{2} \right) D \quad (18)$$

#### IV. EMULATION AND ANALYSIS OF THE OVERALL CELL

##### A. Temp. Effect on bandgap

Since the operating temperature of solar cells in a CPV system can vary widely and become much higher than the ambient temperature, understanding the effect of temperature on solar cell performance is important for CPV system design considerations. As the bandgap decreases, the overall absorption increases and thus the photocurrent of the cell is expected to increase. However, in a multi-junction solar cell, the situation is more complex. The change in bandgap of the top sub-cell, which leads to an increase in its photocurrent, modifies the light spectra available for absorption in the lower lying sub-cells. This change in bandgap depends implicitly on the Varshni parameters. This point becomes clearer when studying the effects of

temperature on the EQE of the device. Furthermore, the benefit of an increased photocurrent is typically dwarfed by the drop in  $V_{oc}$ .

##### B. Temp. Effect on 4-Layer multi-junction solar cells

The effect of the ambient temperature variation from 25°C to 85°C is shown in fig. 5.3 and 5.4 for 4-J solar cell. This figure indicate that the short circuit current is increased slightly as the temperature increases.

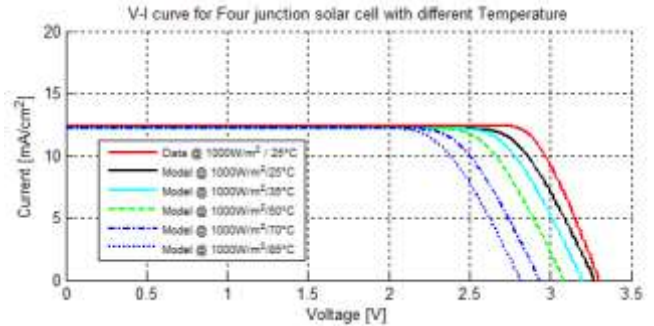


Fig. 6. Temp. Effect on the I-V curve of 4-J solar cell

The 4-J solar cell has the lowest voltage drop when increasing the temperature to 85°C. Fig 5.4 shows the effect of varying

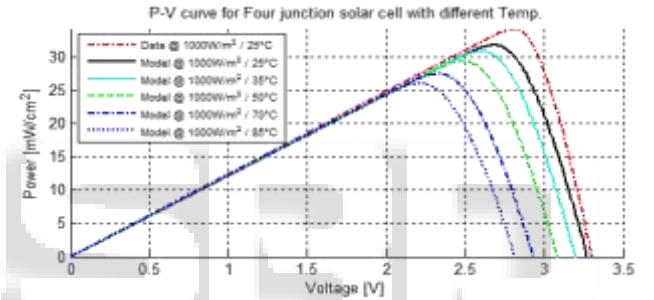


Fig. 7: Temp. Effect on the P-V curve of 4-J solar cell

##### C. Irradiance effect on the 4-layer multi-junction solar cell

It shows that as we temperature increase from 25°C to 85°C, the maximum power of the 4-J solar cell decrease from 40.2mW/cm<sup>2</sup> to 26.3mW/cm<sup>2</sup>. The maximum power of 4-J solar cell reduces due to reduces in the open circuit voltage.

Figure 5.1 show the Voltage versus current density curve with different radiation intensity in which shows that as we increase the radiation intensity of 4-j solar cell, the short circuit current density of solar cells increase significantly while open circuit voltage increase slightly.

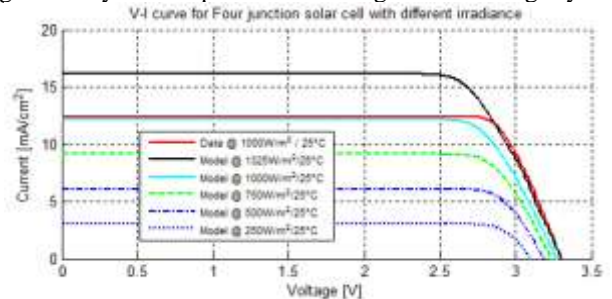


Fig. 8: Irradiance Effect on the I-V curve of 4-J solar cell

When radiation intensity of sun decrease, short circuit current density ( $J_{sc}$ ) decrease significantly while open circuit voltage decrease slightly. Due to change in open circuit voltage and short circuit current density, the maximum power of solar cell reduces as shows in figure 5.2. due to this conversion efficiency of solar cell reduced.

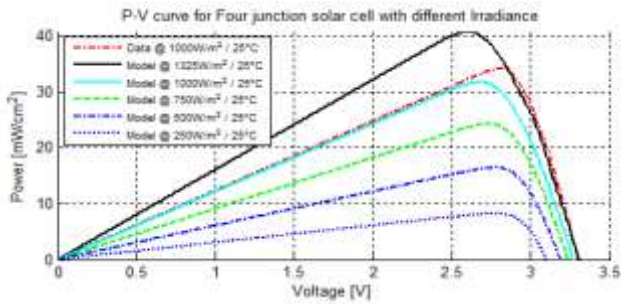


Fig. 9: Irradiance Effect on the P-V curve of 4-J solar cell

D. Comparison with different type of solar cell

The performance of three types of solar cell is compared at standard test conditions i.e., temp. is assumed to be 25°C, solar irradiance is 1000W/m<sup>2</sup>. The comparison includes the I-V and P-V characteristics among different types of solar cells.

The four layer multi-junction solar cells short circuit current density J<sub>sc</sub> is limited by the lowest sub-cell's current conductivity. However, it produced the highest open circuit.

voltage because the load voltage is summation of the voltage produced by each sub-cell taking away the voltage drop across the tunneling diodes and series resistance between them.

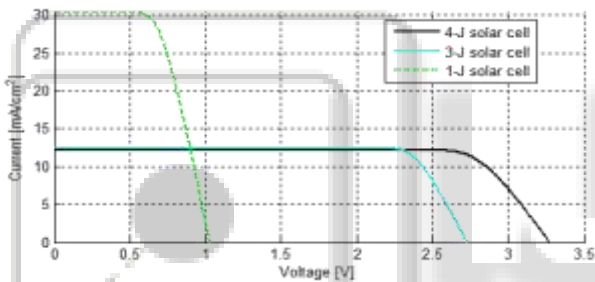


Fig. 10: I-V Curve of Different Type of solar cell: 4-J, 3-J and single junction.

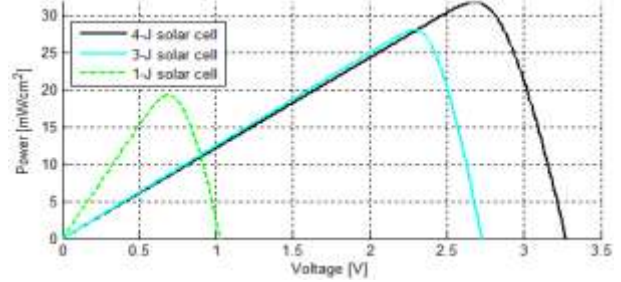


Fig. 11: 4-J, 3-J and single junction P-V curve comparison

By using the fundamental diode equations of solar cell and different material parameter we designed a simulink model as shown in Fig. 12. In this we calculate the cell voltages of each subcells, tunnel diodes voltages between each subcells short circuit current density of each sub cells according to subcells voltage.

We compare four junction solar cell with triple junction and single junction solar cell analysis result as shown in Table II. Here we use standard test parameters such as solar irradiance at 1000 W/m<sup>2</sup> and temp. at 25°C.

Parameters	At standard test Condition [1000W/cm <sup>2</sup> and 25°C]		
	4-J solar cell	3-J solar cell	1-J solar Cell
<b>P<sub>max</sub>[W]</b>	1.76	0.78	0.2
<b>V<sub>oc</sub>[V]</b>	3.302	2.72	1.02
<b>V<sub>max</sub>[V]</b>	2.79	2.3	0.66
<b>J<sub>max</sub>[mA/cm<sup>2</sup>]</b>	12.42	12.6	30.5
<b>Efficiency[%]</b>	33.8	27.01	18.5
<b>Fill Factor[%]</b>	82.9	84.5	82

Table 2: Solar Cell Performance Of 4-J, 3-J And 1-J

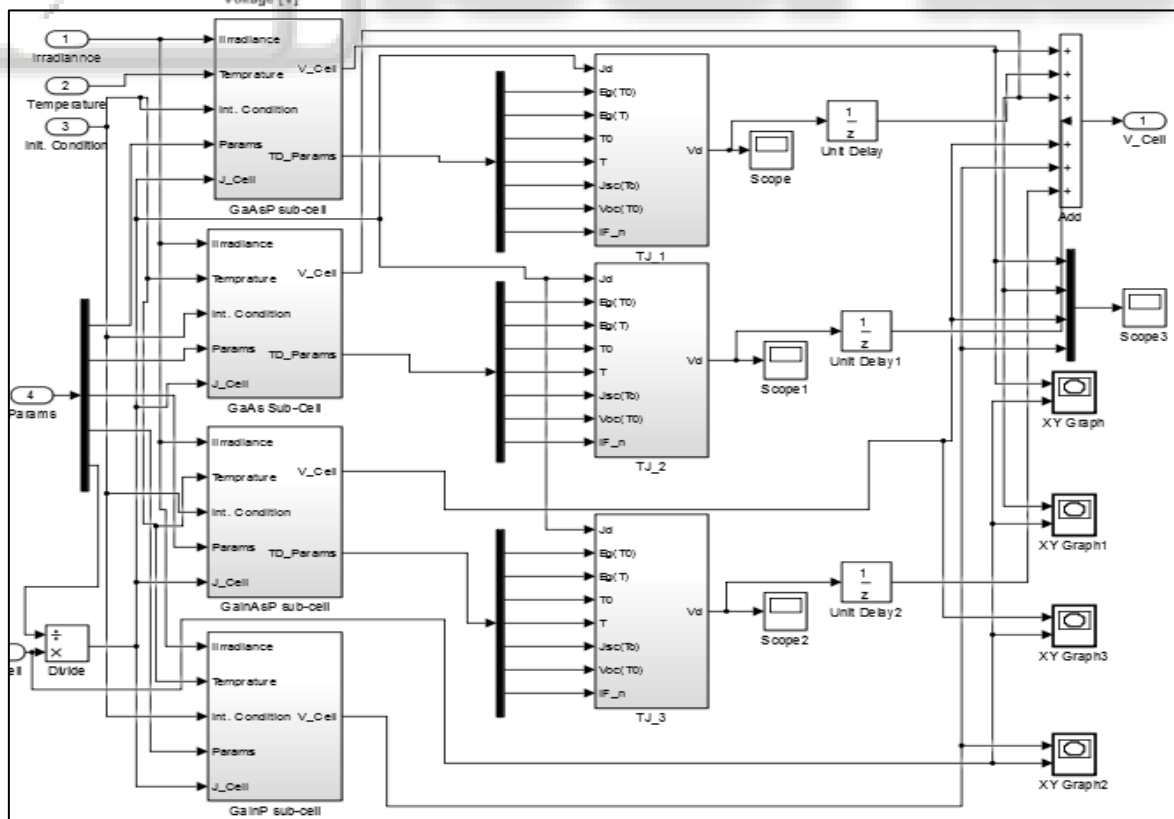


Fig. 12: Main subsystem of 4-j solar cell model implemented in MATLAB/Simulink.

## V. CONCLUSION

When we compare 4-J solar cell characteristics with 3-J and single junction solar cell characteristics using the two diode model. We found that 4-J solar cell is more power efficient than 3-j and single junction. The factors that affected the performance of solar cell are identified and discussed; such as, ambient temperature, solar irradiance, series resistance, and band gap energy. The effects of the factors demonstrated by simulation results of each type of solar cell, and the I-V and P-V characteristics are obtained accordingly. For all types of solar cells, it has found that the temperature increase, short circuit current density  $J_{sc}$  increase slightly while the open circuit voltage decrease significantly. Consequently, the produced electric power decreased with the increasing of cell working temperature. Hence, the produced electric power is increased. For a 4-layer multi-junction solar cell, it shown that the maximum electrical power is directly proportional to the solar irradiance and inversely proportional to the cell working temperature.

## REFERENCE

- [1] Frank Dimroth, Matthias Grave et. Al., "Wafer bonded four-junction GaInP/GaAs//GaInAsP/GaInAs concentrator solar cells with 44.7% efficiency", John Wiley and Sons, Progress in Photovoltaics, Volume 22, Issue 3, pages 277–282, March 2014
- [2] Cornfeld A B, Aiken D, Cho B, et al. Development of a four subcell inverted metamorphic multi-junction highly efficient AM0 solar cell. Photovoltaic Specialists Conference (PVSC), 35th, IEEE, 2010: 000105
- [3] Hauser J R, Carlin Z, Bedair S M. Modeling of tunnel junctions for high efficiency solar cell. Appl Phys Lett, 2010, 97: 04211
- [4] Nishioka K, Takamoto T, Agui T, et al. Evaluation of InGaP /InGaAs/ Ge 3-junction solar cell and optimization of solar cell's structures focusing on series resistance for high efficiency concentrator solar PV systems. Solar Energy Materials, 2006, 90: 1308
- [5] Lu Siyu and Qu Xiaosheng, "AlGaAs/GaAs tunnel junctions in a 4-J tandem solar cell", Journal of Physics, Vol. 32, Nov. 2011.
- [6] Kayes BM, et al., "27.6% conversion efficiency, a new record for single-junction solar cells under 1 sun illumination," in Proc. 37th IEEE Photovoltaic Spec. Conf., 2011, pp. 000004.
- [7] Virshup GF, Chung B-C, Werthen JG. 23.9% monolithic multijunction solar cell. In: Proc. of the 20th IEEE Photovoltaic Specialists Conference, Las Vegas, NV; 1988. p. 441e5.
- [8] Fraunhofer Institute for Solar Energy Systems. World record solar cell with 44.7% efficiency. ScienceDaily. [Online] from <http://www.sciencedaily.com/releases>, [accessed 23.09.12].
- [9] J. F. Geisz, et al., "High-efficiency GaInP/GaAs/InGaAs triple-junction solar cells grown inverted with a metamorphic bottom junction," Appl. Phys. Lett., vol. 91, 2007.
- [10] Shekoofa, O.; Jian Wang," Multi-diode modeling of multi-junction solar cells", IEEE, Electrical

Engineering (ICEE), 2015 23rd Iranian Conference on, May 2015.